Time-lenses for time-division multiplexing of optical OFDM channels

Zihan Geng,[1,*] Bill Corcoran,[1,2] Chen Zhu,[1] and Arthur James Lowery[1,2]

[1]*Department of Electrical and Computer Systems Engineering, Monash University, VIC 3800, Australia*
[2]*Centre for Ultrahigh-Bandwidth Devices for Optical Systems (CUDOS), Australia*
** zihan.geng@monash.edu*

Abstract: Time-lenses provide a promising platform for novel, broadband optical signal processing. However, in order to minimize system penalties, design constraints must be adequately taken into account. We investigate the impact of third-order-dispersion and nonlinear distortion on the performance of time-lens-based communication systems for the first time. Here, we propose a novel application of time-lenses - temporal compression and time-division multiplexing of optical OFDM channels, to provide a 1 Tb/s superchannel. Time-lens system performance degradations are investigated in our proposed system and the results are applicable to all four wave mixing based time-lens systems. Our work can help to optimize time-lens based communication systems.

OCIS codes: (060.2330) Fiber optics communications; (060.4080) Modulation; (070.4340) Nonlinear optical signal processing; (070.1170) Analog optical signal processing.

References and links

1. B. H. Kolner and M. Nazarathy, "Temporal imaging with a time lens," Opt. Lett. **14**(12), 630–632 (1989).
2. R. Salem, M. A. Foster, A. C. Turner, D. F. Geraghty, M. Lipson, and A. L. Gaeta, "Optical time lens based on four-wave mixing on a silicon chip," Opt. Lett. **33**(10), 1047–1049 (2008).
3. B. Li, C. Zhang, J. Kang, X. Wei, S. Tan, and K. K. Y. Wong, "109 MHz optical tomography using temporal magnification," Opt. Lett. **40**(13), 2965–2968 (2015).
4. N. K. Berger, "Generation of long bursts of high-repetition-rate arbitrarily shaped optical pulses using time lens," Opt. Commun. **285**(18), 3855–3863 (2012).
5. O. Kuzucu, Y. Okawachi, R. Salem, M. A. Foster, A. C. Turner-Foster, M. Lipson, and A. L. Gaeta, "Spectral phase conjugation via temporal imaging," Opt. Express **17**(22), 20605–20614 (2009).
6. M. A. Foster, R. Salem, Y. Okawachi, A. C. Turner-Foster, M. Lipson, and A. L. Gaeta, "Ultrafast waveform compression using a time-domain telescope," Nat. Photonics **3**(10), 581–585 (2009).
7. E. Palushani, H. C. H. Mulvad, M. Galili, Hao Hu, L. K. Oxenlowe, A. T. Clausen, and P. Jeppesen, "OTDM-to-WDM conversion based on time-to-frequency mapping by time-domain optical fourier transformation," IEEE J. Sel. Top. Quantum Electron. **18**(2), 681–688 (2012).
8. Y. Xing, Q. Wang, L. Huo, and C. Lou, "Optical time-division demultiplexing using a time-lens-assisted Mach–Zehnder modulator," IEEE Photonics Technol. Lett. **25**(15), 1503–1505 (2013).
9. H. Hu, J. L. Areal, H. C. H. Mulvad, M. Galili, K. Dalgaard, E. Palushani, A. T. Clausen, M. S. Berger, P. Jeppesen, and L. K. Oxenlowe, "Synchronization, retiming and OTDM of an asynchronous 10 Gigabit Ethernet NRZ packet using a time lens for Terabit Ethernet," in *37th European Conference and Exhibition on Optical Communication* (ECOC, 2011), paper Tu.3.K.4.
10. H. Hu, J. L. Areal, E. Palushani, M. Galili, A. T. Clausen, M. S. Berger, L. K. Oxenløwe, and P. Jeppesen, "Synchronization and NRZ-to-RZ format conversion of 10 G Ethernet packet based on a time lens," in *Photonics in Switching,* OSA Technical Digest (Optical Society of America, 2010), paper PMD2.
11. T. Hirooka and M. Nakazawa, "Optical adaptive equalization of high-speed signals using time-domain optical Fourier transformation," J. Lightwave Technol. **24**(7), 2530–2540 (2006).
12. A. J. Lowery, J. Schröder, and L. B. Du, "Flexible all-optical frequency allocation of OFDM subcarriers," Opt. Express **22**(1), 1045–1057 (2014).
13. Y. Li, W. Li, F. Ye, C. Wang, D. Liu, B. Huang, and K. Yang, "Experimental implementation of an all-optical OFDM system based on time lens," Opt. Commun. **284**(16-17), 3983–3989 (2011).
14. H. C. Hansen Mulvad, L. K. Oxenløwe, M. Galili, A. T. Clausen, L. Grüner-Nielsen, and P. Jeppesen, "1.28 Tbit/s single-polarisation serial OOK optical data generation and demultiplexing," Electron. Lett. **45**(5), 280–281 (2009).

#248812 Received 28 Aug 2015; revised 21 Oct 2015; accepted 28 Oct 2015; published 5 Nov 2015

15. C. V. Bennett and B. H. Kolner, "Aberrations in temporal imaging," IEEE J. Quantum Electron. **37**(1), 20–32 (2001).
16. A. J. Lowery and L. B. Du, "Optical orthogonal division multiplexing for long haul optical communications: A review of the first five years," Opt. Fiber Technol. **17**(5), 421–438 (2011).
17. W. Shieh, H. Bao, and Y. Tang, "Coherent optical OFDM: theory and design," Opt. Express **16**(2), 841–859 (2008).
18. J. Armstrong and A. J. Lowery, "Power efficient optical OFDM," Electron. Lett. **42**(6), 370–372 (2006).
19. B. H. Kolner, "Generalization of the concepts of focal length and f-number to space and time," J. Opt. Soc. Am. A **11**(12), 3229–3234 (1994).
20. H. C. H. Mulvad, H. Hu, M. Galili, H. Ji, E. Palushani, A. T. Clausen, L. K. Oxenløwe, and P. Jeppesen, "DWDM-to-OTDM conversion by time-domain optical Fourier transformation," in *37th European Conference and Exhibition on Optical Communication* (ECOC, 2011), Geneva, Switzerland, paper Mo.1.A.5.
21. M. A. Foster, R. Salem, D. F. Geraghty, A. C. Turner-Foster, M. Lipson, and A. L. Gaeta, "Silicon-chip-based ultrafast optical oscilloscope," Nature **456**(7218), 81–84 (2008).
22. P. Guan, D. Kong, K. M. Røge, H. C. H. Mulvad, M. Galili, and L. K. Oxenløwe, "Real-time all-optical OFDM transmission system based on time-domain optical fourier transformation," in *Optical Fiber Communication Conference,* Technical Digest (optical Society of America, 2014), paper W4F.1.
23. V. Torres-Company, J. Lancis, and P. Andrés, "Spectral imaging system for scaling the power spectrum of optical waveforms," Opt. Lett. **32**(19), 2849–2851 (2007).
24. E. Palushani, H. C. H. Mulvad, D. Kong, P. Guan, M. Galili, and L. K. Oxenløwe, "All-optical OFDM demultiplexing by spectral magnification and band-pass filtering," Opt. Express **22**(1), 136–144 (2014).
25. A. W. Lohmann and D. Mendlovic, "Temporal filtering with time lenses," Appl. Opt. **31**(29), 6212–6219 (1992).
26. Y. Okawachi, R. Salem, M. A. Foster, A. C. Turner-Foster, M. Lipson, and A. L. Gaeta, "High-resolution spectroscopy using a frequency magnifier," Opt. Express **17**(7), 5691–5697 (2009).
27. H. C. H. Mulvad, E. Palushani, H. Hu, H. Ji, M. Lillieholm, M. Galili, A. T. Clausen, M. Pu, K. Yvind, J. M. Hvam, P. Jeppesen, and L. K. Oxenløwe, "Ultra-high-speed optical serial-to-parallel data conversion by time-domain optical Fourier transformation in a silicon nanowire," Opt. Express **19**(26), B825–B835 (2011).
28. A. J. Lowery, "Amplified-spontaneous noise limit of optical OFDM lightwave systems," Opt. Express **16**(2), 860–865 (2008).
29. OFS datasheet, "HNLF zero-slope, HNLF zero-slope highly non-linear fiber modules," *http://fiber-optic-catalog.ofsoptics.com/item/optical_fibers/highly-nonlinear-fiber-optical-fibers1/hnlf-zero-slope-highly-non-linear-fiber-modules* (OFS, 2015)

1. Introduction

Optical time-lenses [1] provide a method to transform the temporal and spectral properties of pulses. These systems are useful tools for short pulse analysis [2], bandwidth enhancement of medical imaging systems [3] and the generation of arbitrary optical waveforms [4, 5]. Time-lenses provide a temporal domain analogue to physical lenses through the application of chirp and chromatic dispersion to optical waveforms. This allows for the exchange of information to and from the spectral and temporal domains via all-optical Fourier transformation, and temporal magnification and compression [6]. The ability to scale and exchange the temporal and spectral information of optical waveforms is of particular interest to the manipulation of optical signals in communication systems.

Time-lens sub-systems have become useful components for different all-optical signal processing applications in optical communications, with demonstrations of the conversion of time-to-wavelength division multiplexed signals [7], optical time-division demultiplexing [8], retiming and synchronization of optical signals [9], format conversion [10], mitigation of linear channel impairments [11], indicating the range of potential uses of these devices in communication systems. The ability to transform optical signals to and from a variety of multiplexing formats and baud rates is of interest when considering interchanges in heterogeneous optical networks. The manipulation of spectrally efficient optical super-channels [12, 13] is of particular interest, since this is difficult to do using traditional methods. Moreover, time-lens systems processing large bandwidths may provide more efficient signal processing than multiple parallel optical-electrical-optical stages [14].

In order to efficiently process broad optical bandwidths, nonlinear optical effects such as four wave mixing are often used to provide the key chirping step needed in time-lens systems. Ideally a linearly chirped control pulse will transfer its chirp to the target signal, which when combined with group velocity dispersion in an optical fiber, can produce the desired time-lens

#248812 Received 28 Aug 2015; revised 21 Oct 2015; accepted 28 Oct 2015; published 5 Nov 2015

function. Practically, these systems are limited by the achievable pulse shapes for the control pulse, higher order nonlinear mixing and higher order chromatic dispersion contributions which can provide distortions to the time-lens function. Ultimately, these effects degrade the processed signal. While these degradations have been investigated in terms of the manipulation of Gaussian pulses [15], their impact on signals carrying optical data has not been well explored.

Here we investigate the use of temporal compression to time-division multiplex spectrally efficient optical orthogonal frequency division multiplexed (OFDM) [16–18] signals. We present a time-lens based sub-system to combine low-symbol rate OFDM tributaries into a higher baud rate channel, providing a test case to probe the limitations of time-lenses for all-optical signal processing. This investigation provides the first thorough performance characterization of the impact of non-ideal time-lens system parameters on optical data, in terms of the widely used digital communication metric of signal quality factor (Q). We show that the system can provide close to ideal performance using selected off-the-shelf components.

Through numerical modelling of a practically achievable, four-wave mixing (FWM) based time-lens system, we isolate and quantify the impact of higher-order nonlinear and dispersive distortions on the processed data symbols, and we find that the performance of the time-lens-based sub-system is primarily limited by distortions to signal chirping from the dispersion slope in highly nonlinear fiber.

2. Time-lens based symbol compression for time division multiplexing

As shown in Fig. 1, a time-lens is a temporal analogue to a physical lens, where chromatic dispersion and temporal chirp provide a mathematically identical effect on an optical waveform in the time domain to the effect of physical lens on an optical wavefront in space [19]. In a physical lens system, the wavefront diffracts and so that it is spatially dispersed as it travels, while the lens provides a phase change on the wavefront that is dependent on position, generating a spatial chirp. In a time-lens system, diffraction is emulated by chromatic dispersion, spreading a temporal waveform out in time. The spatial chirp as generated by the physical lens is substituted for a temporal chirp. A time-lens can be constructed using two dispersive elements, such as dispersive optical fiber, and a device to impart a linear temporal chirp.

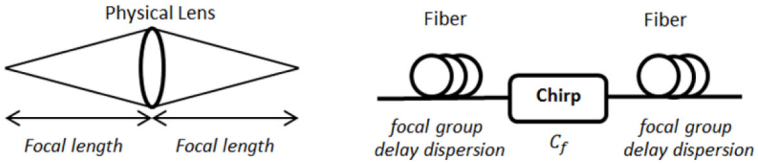

Fig. 1. Analogue between physical lens and time-lens. Input and Output dispersions act as free-space diffraction. Temporal chirp plays the role of spatial chirp.

The ‘focal length’ of a time-lens is defined by the chirp applied to the optical waveform [19]. In order for this lens system to focus, the temporal waveform needs to undergo an equivalent dispersion, such that the applied chirp (C_f [Hz/s]) is inversely proportional to the accumulated dispersion ($\beta_2 L_f$), with the focal group delay dispersion defined as $\phi_f = 1/(2\pi C_f) = \beta_2 L_f$ (where β_2 is the group-velocity dispersion parameter of the dispersive fiber, and L_f is the length of that fiber) [2].

The dispersion required for a time-lens can be imposed by dispersive fiber, and the linear temporal chirp is commonly achieved by mixing the input waveform with a linearly chirped optical pulse via FWM in highly nonlinear fiber. As FWM is produced via the ultrafast Kerr effect, its response time is in the order of femtoseconds. Moreover, highly nonlinear fibers can

#248812 Received 28 Aug 2015; revised 21 Oct 2015; accepted 28 Oct 2015; published 5 Nov 2015

be engineered to allow for phase matching over large bandwidths. As such, FWM-based time-lenses can support real-time and broadband optical signal processing.

As with physical lenses, a time-lens can be used for a multitude of applications. A time-lens can produce an output temporal waveform which is the time-domain Fourier transform of the input waveform. The Fourier transform property has been used for applications such as DWDM-to-OTDM conversion [20], ultrafast optical oscilloscope [21], and optical OFDM generation [22]. Other combinations of time-lenses enable temporal or spectral scaling, which has provided ultrafast waveform compression [6] and spectral magnification [23, 24].

The time-lens system numerically derived in [25] provides scaling in both temporal and spectral domain. This system will be called a "time-lens pair" in this paper. As shown in Fig. 2, a time-lens pair is composed of two time-lenses. By using different chirp rates in the two time-lenses, the temporal pulse and power spectra of the input signal can be compressed or magnified, analogous to a spatial system using two lenses with different focal lengths. ϕ_{f1} and ϕ_{f2} are the focal group delay dispersions of the first and second time-lens, respectively. The output waveform of the time-lens pair is scaled replica of the input waveform, with the scaling factor is given by $K = \phi_{f1}/\ \phi_{f2}$. This configuration is used as it provides Fourier transform-limited compression of the incoming waveform, such that the product of the symbol duration ($\Delta\tau$) and spectral widths (Δf) of the incoming signal remains at a single value (i.e. $\Delta\tau_{in} \times \Delta f_{in} = \Delta\tau_{out} \times \Delta f_{out}$). This property is not provided by the 'spectral imaging' type time-lens [23, 24].

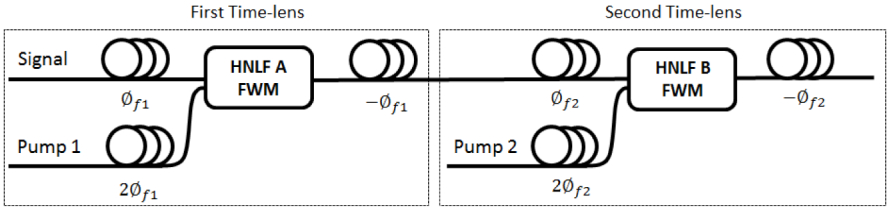

Fig. 2. Schematic of a time-lens imaging system. The first time-lens converts OFDM to Nyquist-OTDM, and the second time-lens converts the signal to spectrally magnified OFDM.

In this paper, we propose a novel application of a time-lens pair, using temporal compression and aggregation of OFDM symbols to provide optical time-division multiplexing (OTDM) of OFDM symbols. Figure 3 shows the principle. The compression block in Fig. 3, refers to the time-lens pair shown in Fig. 2. Stream A and Stream B are two OFDM channels; each symbol within each channel is compressed in time by a pair of time-lenses. Stream B is delayed by half of the bit period.

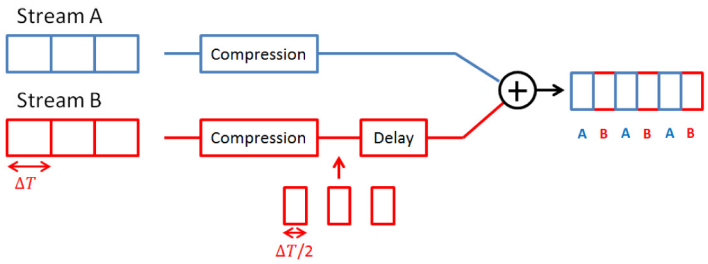

Fig. 3. Schematic of Time Division Multiplexing of time-lens compressed OFDM streams. Two OFDM channels are separately compressed by time-lenses and then time-interleaved.

The compression creates gaps in the waveforms of each channel, allowing the channels to be time interleaved. In this way, several channels of OFDM symbols could be combined into a single data stream. The number of channels that can be time-division multiplexed is limited by the compression ratio of two time-lenses. In our simulations, five OFDM channels are

#248812 Received 28 Aug 2015; revised 21 Oct 2015; accepted 28 Oct 2015; published 5 Nov 2015

combined into one data stream to investigate time-lens based OTDM of OFDM. This is a complex system, which requires synchronized inputs and pumps over10 time-lens pairs. The bandwidth requirements for this system do, however, make it suitable for the investigation of penalties that arise from non-idealities present in practically achievable time-lens systems.

3. Time-lens design guidelines

The performance of the time-lens pair is affected by some constraints. The time-lens pair is constrained by a limited temporal 'record window', a limited spectral capture range, aberrations from third order dispersion (TOD) and practical limits on the chirping 'pump' pulse shape.

In the FWM process, the signal would be chirped only in the time slots in which a pump pulse is present [21]. This leads to a limited temporal record window, defined by the temporal duration of the chirping pump pulse, and can be approximated by

$$t_{record} = 4\pi\phi_f \Delta f_{pump} \tag{1}$$

where Δf_{pump} is the bandwidth of the pump used to impart chirp on the input optical waveform. To work within this limitation, the input OFDM symbol length should be shorter than the record window of the first time-lens. In addition, the chirp rate of the first time-lens should be properly chosen to make the time-domain symbol length of the first time-lens output smaller than the record window of the second time-lens. The output signal time-domain symbol length of first time-lens is given by input signal bandwidth divided by the chirp rate C_1, where $C_1 = 1/(2\pi\phi_{f1})$.

Related to the record window is a limitation on the input spectral bandwidth that is able to be processed by the time-lens pair [26]. If the above mentioned record window condition is fulfilled, the maximum possible bandwidth of the input spectrum that can be processed by time-lens is given by

$$\Delta f_{in} = \left| \frac{C_1}{C_2} 2\Delta f_{pump2} \right| = \left| \frac{\phi_{f2}}{\phi_{f1}} 2\Delta f_{pump2} \right| \tag{2}$$

where Δf_{pump2} is the pump bandwidth of the second time-lens [2]. We can regard the process in the first time-lens frequency-to-time conversion and the process in the second time-lens time-to-frequency conversion. Since the record window of the second time-lens ($4\pi\phi_{f2}\Delta f_{pump2}$) is finite, the frequency components converted from the temporal waveform at the input of the second time-lens are limited in bandwidth. The input and output of the first time-lens follow the relationship $\Delta f_{in} = \Delta t_{out1}/2\pi\phi_{f1}$, where Δf_{in} is the full-width at half-maximum (FWHM) of the input signal's spectrum and Δt_{out1} is FWHM of the output of the first time-lens. This then leads to the restriction given by Eq. (2). When a time-lens is used to process signals with wide bandwidths — as is the case with the sinc 'tails' of an OFDM spectrum — the frequency components far from the center frequency of the signal will be lost. In order to keep enough frequency information to prevent significant signal distortion, the bandwidth of Pump 2 must exceed a minimum value.

From the analysis above, a broader pump bandwidth implies a longer record window and a wider maximum spectral range. However, if the bandwidth of the pump is excessively large, third-order dispersion can distort the FWM nonlinear mixing process, limiting the maximum useful pump bandwidth. It has been previously stated that for Gaussian pulse inputs to a time-lens, perturbations (or aberrations) to the output signal due to third-order dispersion can be ignored if the dispersion effects of β_2 greatly outweigh those of β_3 [15].

Ideally, the pump pulses should be rectangular and the chirp of the pump should be linear; however, in practical systems the pump pulses will have gradual rising and falling edges. The edges of pump pulses often have non-linear chirp and will have reduced power compared with

#248812 Received 28 Aug 2015; revised 21 Oct 2015; accepted 28 Oct 2015; published 5 Nov 2015

the predominantly flat, constant power, linearly chirped, middle part. As such, any part of the signal that overlaps with pump edges will experience severe spectral and temporal distortion [27]. The distortion from these edges will lead to reduced symbol compression, and so to inter-symbol-interference when time division multiplexing the compressed pulses. Thus, maximizing the overlap between the signal and the flat-top middle of the pump is important when optimizing a time-lens system.

The pump pulses' edges pose problems if the time-lens is to operate continuously in the time domain. To avoid this problem, the repetition rate of the pump is set to half of the baud rate of the signal, with the signal temporally interleaved to create two parallel streams of odd and even symbols. The odd and even symbols are then processed separately in two time-lens pairs. This allows the signal to be aligned to the middle of the pump pulse to mix only with the flat, linearly chirped part of the pump pulse.

Further complications arise from symbol temporal broadening due to the focal group delay dispersion fiber (i.e. Fiber 1 in Fig. 4) placed before the first FWM stage. The amount of broadening is dependent upon the length of the dispersive fiber, and is inversely proportional to the chirp rate of the first time-lens. Thus a lower chirp rate means more temporal symbol broadening in Fiber 1. This then limits the minimum bandwidth that the pump pulses can take, providing a lower bound, in contrast to the upper bound defined by third order dispersion.

By observing the limitations outlined above, it is often possible to tailor a time-lens systems to the required signal processing application. However, in some cases these sources of distortion can be a fundamental limiting factor.

4. Numerical simulations and results

We used VPItransmissionMaker to simulate a five tributary system, as shown in Fig. 4.

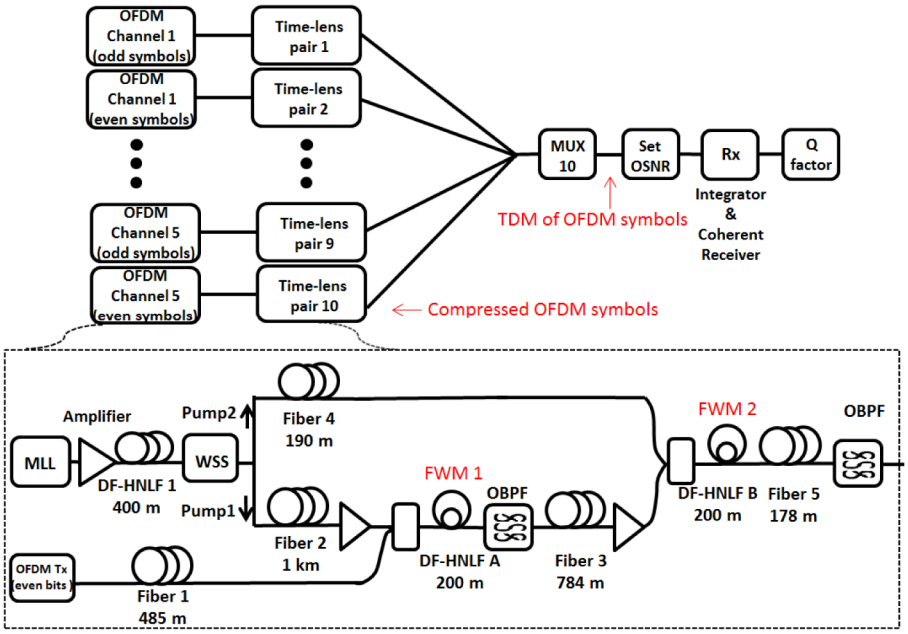

Fig. 4. Simulation setup of time division multiplexing five 5-subcarrier OFDM tributaries with quadrature phase-shift keying (QPSK).

At the transmitter, there are five OFDM channels, all with a center wavelength of 1552.5 nm (193.1 THz). As mentioned in Section 3, each channel is temporally interleaved into odd and even symbol tributaries. Each OFDM channel has five 20 Gbaud QPSK subcarriers with a

#248812 Received 28 Aug 2015; revised 21 Oct 2015; accepted 28 Oct 2015; published 5 Nov 2015

20-GHz subcarrier spacing, providing a line rate of 200 Gb/s per channel. The aggregate line rate of these channels is then 1 Tb/s.

Linearly chirped pump pulses are generated from short Gaussian pulses via self-phase modulation and dispersion. The mode-locked laser (MLL) produces 1.5-ps wide Gaussian pulses at 10 Gpulses/s centered at 1534.2 nm (195.4 THz). The Gaussian pulses are amplified to 0.2-W average power, and then spectrally broadened in dispersion flattened highly nonlinear fiber (DF-HNLF 1). The amplified spontaneous emission (ASE) noise of amplifiers is set to zero in the simulation. Third-order dispersion in all the fibers is set to zero at this stage. The effect of TOD will be discussed in Section 5. DF-HNLF 1 is 400-m long with a dispersion of −1.2 ps/nm/km and a nonlinear index of 10 $W^{-1}km^{-1}$. After DF-HNLF 1, a wavelength selective switch (WSS) is simulated as implementing two 5th-order Gaussian optical filters to produce two pumps with flat top spectra. The Gaussian filter bandwidth for Pump 1 is 360 GHz and is 1.3 THz for Pump 2. Pump 1 is linearly chirped using 1-km of dispersion compensating fiber (DCF) (Fiber 2) with −30 ps/nm/km dispersion, while Pump 2 is chirped in a 190-m DCF (Fiber 4). This produces a chirp rate of 9.2×10^{21} Hz/s in the first (DF-HNLF A) and 4.6×10^{22} Hz/s in second (DF-HNLF B) signal chirping stages. Note that the ratio of the applied chirps is 5, so the time-lens pair provides a factor 5 spectral magnification and temporal compression.

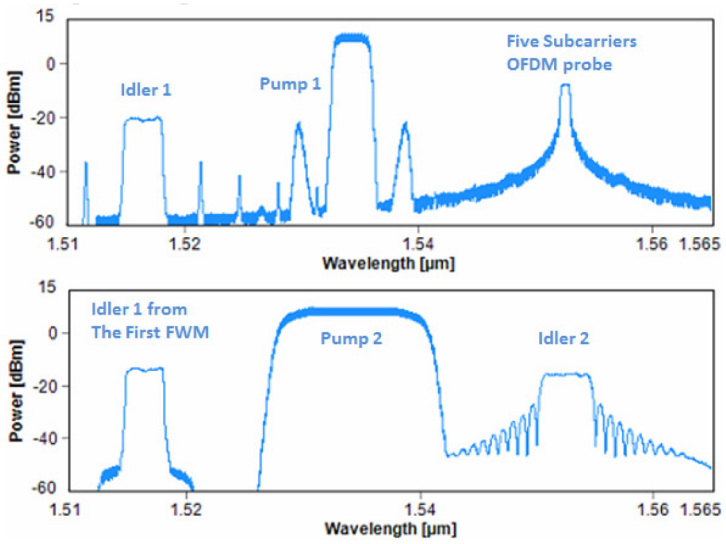

Fig. 5. (Top) optical spectra after the first time-lens; (Bottom) optical spectra after the second time-lens.

The even (or odd) symbols of one OFDM channel are dispersed in 485-m DCF (Fiber 1) with −30 ps/nm/km dispersion. Due to the FWM process in 200-m highly nonlinear fiber (DF-HNLF A), the chirped pulse and the input signal mix to produce an idler (Idler 1) that is strongly chirped. To reduce pump-signal walk-off in highly nonlinear fiber, high pump power and short fiber length are used. An optical band pass filter filters out the idler (Idler 1) generated due to FWM process in DF-HNLF A. Idler 1 is linearly chirped and has the same intensity waveform as the input OFDM symbols. After propagation in 784 m of single mode fiber (SMF - Fiber 3), Idler 1 is combined with Pump 2 in DF-HNLF B to produce a highly chirped idler (Idler 2). Idler 2 is dispersed in a 178 m of SMF (Fiber 5) and compressed OFDM symbols are generated. Both the DF-HNLFs have a nonlinear index = 10 $W^{-1}km^{-1}$, are 200m long and have a zero dispersion centered at 1534 nm. The average powers of Pump 1 and Pump 2 are set to 23 dBm and 28 dBm respectively. In this case, signal output power is equal to the signal input power (i.e. 0 dBm), and the input signal data quality can be

#248812 Received 28 Aug 2015; revised 21 Oct 2015; accepted 28 Oct 2015; published 5 Nov 2015

preserved. Figure 5 shows the optical spectra after the two FWM processes. All of the five OFDM channels processed as described above simultaneously. The delays assigned to the 10 compressed OFDM symbol trains are 0 ps, 10 ps, 20 ps etc. Figure 6 shows that the original symbols are compressed after the ten parallel time-lens pairs and time division multiplexed.

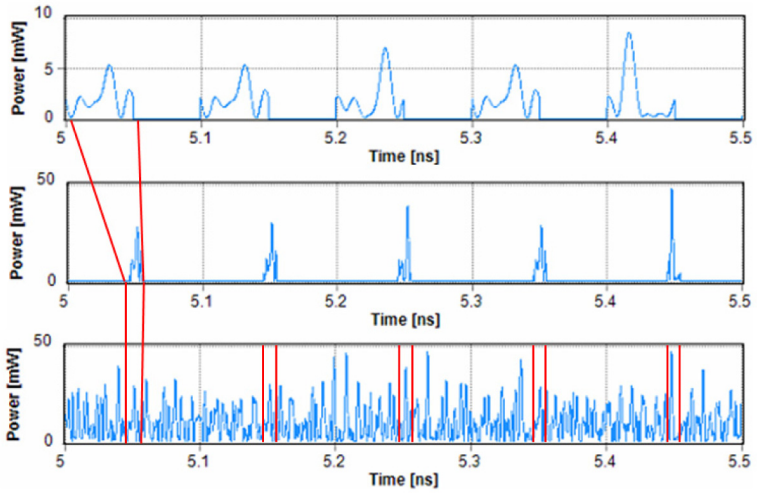

Fig. 6. (Top)Waveform of original signal; (Middle) Waveform of signal compressed by time-lenses; (Bottom) Waveform of the time division multiplexed five OFDM channels.

Each subcarrier is demultiplexed using a matched filter with a sinc frequency response (a rectangular time response). To receive the QPSK modulated signal, a coherent receiver is used here to detect the amplitude and phase of the signal. The five channels are selected by sampling in their corresponding time slots.

A typical received signal is shown in Fig. 7. There are five eyes every 50 ps, which indicate that the five OFDM channels have been time division multiplexed successfully. Each of the five eyes corresponds to one OFDM channel. By sampling at corresponding position, each channel's information can be decoded.

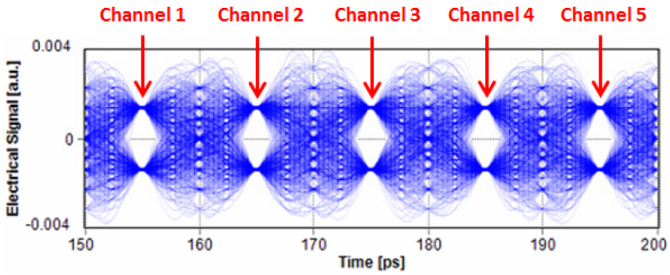

Fig. 7. Eye diagram of an OFDM subcarrier at receiver on I phase.

Figure 8 shows the signal quality, *Q,* versus the optical signal-to-noise ratio (OSNR) of 5-channel OTDM OFDM signal and the associated theoretical upper bound to performance [28]. In Fig. 8, the comparison between the OFDM signals composed by 5 compressed OFDM channels and the theoretical upper bound indicates the simulated time-lens system performance is close to ideal. When the optical signal-to-noise ratio (OSNR) is 40 dB, the Q-factor degradations for all the subcarriers are less than 0.5 dB.

#248812 Received 28 Aug 2015; revised 21 Oct 2015; accepted 28 Oct 2015; published 5 Nov 2015

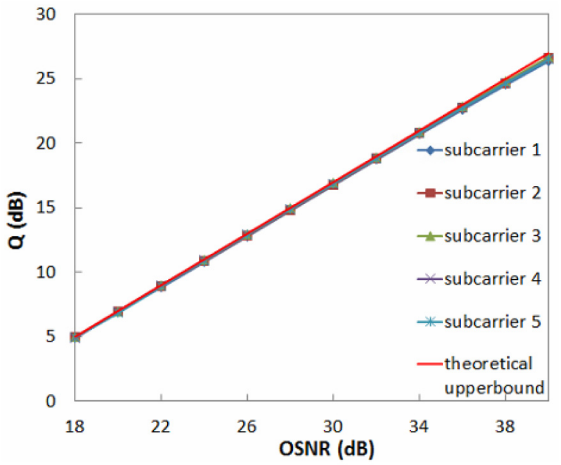

Fig. 8. Q vs. OSNR of TDM of 5 time-lenses compressed OFDM channels.

5. System penalty analysis

The results in Section 4 are for a system with close to ideal operating conditions. We will now investigate some of the parameters that may limit the system performance, and show that nonlinear distortion and third order dispersion are the major sources of aberration in the time-lens pair that we simulate.

5.1 Nonlinear effects

In the DF-HNLF A and DF-HNLF B, the signal is highly chirped by mixing with the linearly chirped pumps. However nonlinear effects also cause aberrations in time-lens. Self-phase modulation (SPM) changes the phase of pumps and broadens the spectrum of pumps. Cross-phase modulation (XPM) causes unwanted mixing between pump, signal and idler. FWM within the pump pulse is caused by temporal overlapping of sequential pump pulses and generates undesired frequency components. FWM among the five OFDM subcarriers also generates unwanted nonlinear mixing terms.

To investigate the effect of nonlinear distortion, the effects of other distortion sources should be minimized. Therefore the third-order dispersion and power amplifier noise are set to zero in our simulation. As shown in Fig. 8, if the power of signal and pump and highly nonlinear fiber length are properly chosen, close to ideal performance can be achieved.

The effects of signal power, Idler 1 power, Pump 1 power and Pump 2 power are explored. For simplicity, only the results of center subcarrier (193.1 THz) are shown in Fig. 9. The default values are: signal average power = 0 dBm, Pump 1 average power = 23 dBm, Pump 2 average power = 28 dBm. Only one of the three powers is changed at any one time, while other two powers are set to default values. The signal under test is the same as in Section 4.

Figure 9(a) suggests that lower signal input power should be used in this system, to avoid nonlinear distortion. However, in order to get a certain output power, the input power should exceed a certain level, otherwise an amplifier should be used at the end of time-lens pair and amplifier noise will add to the signal. In Fig. 9(b), the performance trend, when varying the power of Idler 1 at the input to the second time-lens, has the similar effect to varying signal power at the input of the first time-lens, because Idler 1 is the "signal" in the second four wave mixing process. When the signal power and Pump 1 power are set to default values, the Idler 1's power is –6.5 dBm.

Figures 9(c) and 9(d) show how the received signal quality and power varies with changing of pump power. In order to minimize the penalty due to power loss in the first time-

#248812 Received 28 Aug 2015; revised 21 Oct 2015; accepted 28 Oct 2015; published 5 Nov 2015

lens (and hence noise from a required amplifier stage), 0 dBm output power is desired and so Pump 1 power is set to 23 dBm in our simulation. This provides only moderate distortion due to nonlinear cross-talk in the first time-lens. In Fig. 9(d), the Q-factor is roughly constant for Pump 2 average powers lower than 30 dBm, dropping dramatically for higher pump powers. Therefore, the output power of Pump 2 should be kept below 30 dBm. Conveniently, an average Pump 2 power of 28 dBm provides 0 dB conversion efficiency in the second time-lens, so an overall 0 dB conversion efficiency over the time-lens pair is possible without incurring significant nonlinear penalty.

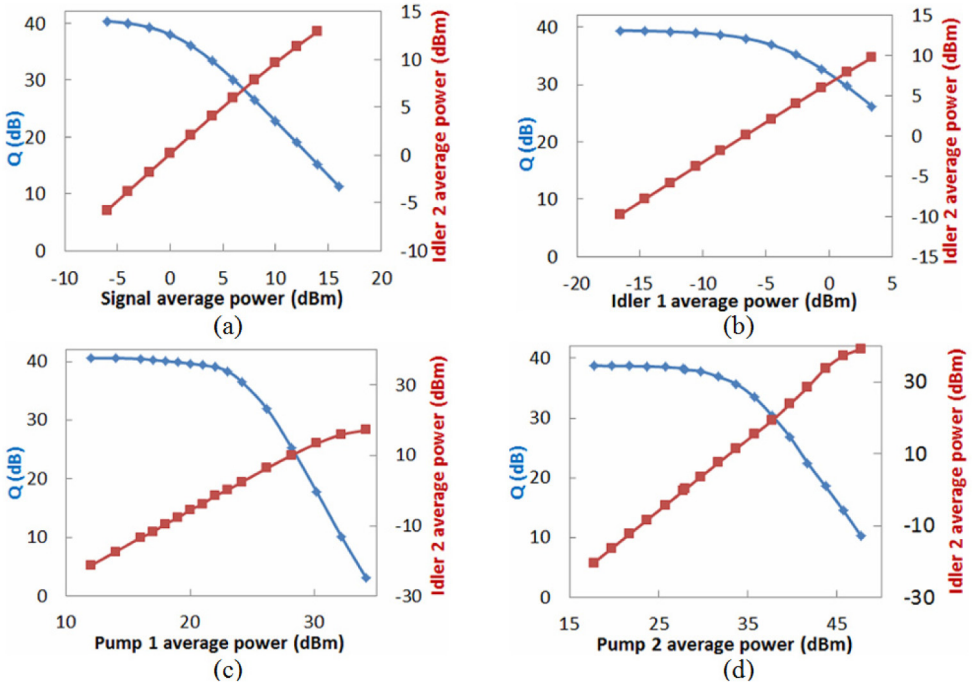

Fig. 9. Q factor vs. system parameters (a) Q factor vs. signal average power. (b) Q factor vs. Idler 1 power. (c) Q factor *vs*. Pump 1 average power. (d) Q factor vs. Pump 2 average power. Red represents Idler 2 average power. Blue represents Q factor.

To identify the source of the degradation due to unwanted nonlinear interactions as shown in Fig. 9, the optical spectra at the output of DF-HNLF A (left column) and DF-HNLF B (right column) are shown in Fig. 10. In this figure, the average powers of the two pump pulses and the signals at the input of the two separate time-lenses are varied. Figures 10(a) and 10(b) show the output spectra in the case of a signal power that is too high. Figures 10(c), 10(d), 10(e) and 10(f) are for Pump 1's power being too high. Figures 10(g) and 10(h) are for Pump 2 power's power being too high.

In Figs. 10(a) and 10(b), the signal power input to DF-HNLF A is 16 dBm, Pump 1 is 23 dBm and Pump 2 is 28 dBm. In this case, when the signal (right) and Pump 1 (middle) powers are similar, the top of the Pump 1 spectrum at DF-HNLF A output is no longer flat. When combined with the Idler 2 output power trend in Fig. 9(a), we infer that the penalty from increasing signal is not due to pump depletion, but is due to nonlinear mixing distorting both the original signal and the pump. In Fig. 10(b), the spectrum of Idler 2 (right) is not typical of an OFDM signal, indicating significant distortion. Therefore, as shown in Fig. 9(a), the input signal power should well below the pump power to avoid unwanted nonlinear interactions.

As shown in Figs. 10(c) and 10(d), when Pump 1 is set to 33 dBm, the power of Idler 1 at the input of second time-lens (i.e. into DF-HNLF B) is high (13.5 dBm average power). This

#248812 Received 28 Aug 2015; revised 21 Oct 2015; accepted 28 Oct 2015; published 5 Nov 2015

is well into the nonlinear distortion regime of Fig. 9(b), and as such, the output spectra of DF-HNLF B shown in Figs. 10(b) (high signal input) and 10(d) (high Pump 1 input) shows distortion of Pump 2 spectrum.

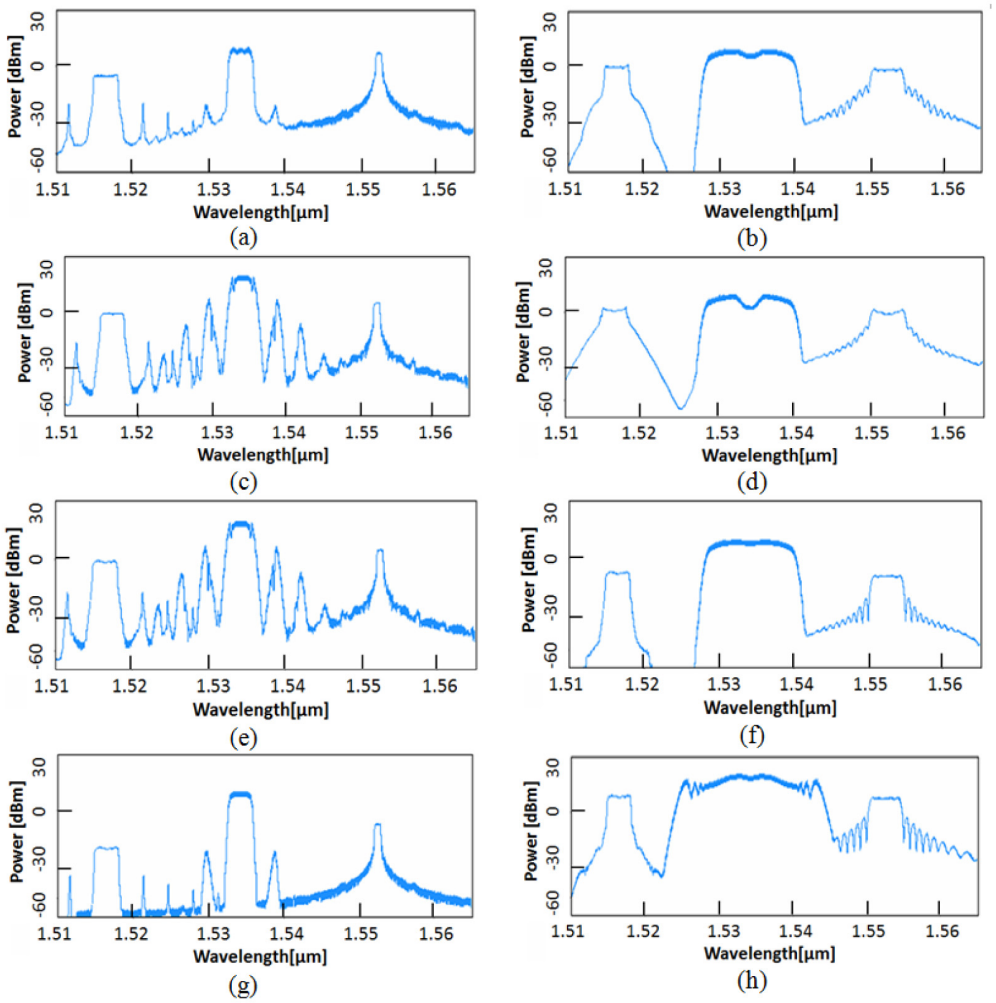

Fig. 10. Spectra at output of DF-HNLF A (left) and DF-HNLF B (right) under the conditions (a) and (b): 16-dBm signal power, 23-dBm Pump 1 power, 28-dBm Pump 2 power; (c) and (d): 0-dBm signal power, 33-dBm Pump 1 power, 28-dBm Pump 2 power; (e) and (f): 0-dBm signal power, 33-dBm Pump 1 power, 28-dBm Pump 2 power, with Idler 1 attenuated by 14 dB; (g) and (h): 0-dBm signal power, 23-dBm Pump 1 power, and 40-dBm Pump 2 power.

The operating condition for Figs. 10(e) and 10(f) is similar to Figs. 10(c) and 10(d), except that Idler 1 is attenuated by 14 dB (to –0.5 dBm average power) before the FWM process in DF-HNLF B. A clear OFDM spectrum can be seen in Fig. 10(f) and the quality factor of the received signal is 29 dB. Compared with Fig. 10(f), the degradation in Fig. 10(d) is primarily due to nonlinear distortion from having a too high Idler 1 power at the input to DF-HNLF 2, as opposed to resulting from nonlinear chirp due to the distorted Pump 1 pulse.

In Figs. 10(g) and 10(h), the average power of Pump 2 is increased to 40 dBm. As shown in Fig. 10(h), this results in a spectral broadening of Pump 2, which we infer to cause a nonlinear chirp on Idler 2, resulting in a degraded output signal. However, there is no drastic perturbation to the spectrum of Idler 2, even though the signal quality factor falls to 26 dB.

#248812 Received 28 Aug 2015; revised 21 Oct 2015; accepted 28 Oct 2015; published 5 Nov 2015

Comparing Figs. 10(g) and 10(h), we note that the input Idler 1 seems to undergo parametric amplification.

Figure 10(g) shows the spectrum out of DF-HNLF A when the powers of signal and Pump 1 are properly chosen to minimize nonlinear distortion (i.e. 0 dBm and 23 dBm respectively). Notably, there are two spurious frequency components generated, appearing as frequency 'spikes' around Pump 1. The spikes are caused by the temporal overlap of pump pulses. Ideally, the pump pulses would not overlap, however in order to generate a constant chirp over the symbol duration after the signal undergoes focal dispersion, the leading and falling edges of the pumps do slightly overlap. Because of the way that the pump pulses are chirped, the leading edge corresponds to the lowest frequency components of the pump and the tailing edge corresponds to the highest frequency components of the pump. The two spikes are the FWM products of the two spectral edges of the pump. The distance between the left spike and the left edge is equal to the bandwidth of Pump 1, which holds for the right edge and spike. As shown in Figs. 10(c) and 10(e), when the power of Pump 1 is large, not only do the two spikes closest to Pump 1 become larger, more spikes appear around Pump 1 due to higher-order FWM. If the spikes overlap with desired signal spectrally, the received data will be distorted. There is no spike close to Pump 2 because its bandwidth is tailored to avoid temporal pulse overlap.

5.2 Third order dispersion

Third-order dispersion must be taken into consideration when broad pump bandwidth is used. The dispersion slopes of Fiber 3 and Fiber 5 are set to 0.092 ps/nm^2/km, as for standard SMFs, while the dispersion slopes of DF-HNLF A and DF-HNLF B are set to 0.006 ps/nm^2/km, which is typical of some DF-HNLFs [29]. We can then have these effects included in the simulated performance of the time-lens pair. From Fig. 11, we can see that the dispersion slope causes some performance penalty, degrading Q by about 4 dB at high OSNRs (40 dB). This trend is almost unchanged if the dispersion slope is eliminated in the SMF and DCF sections of the time-lens pair, indicating that the slope of the DF-HNLF is the major cause of the degradation shown in Fig. 11.

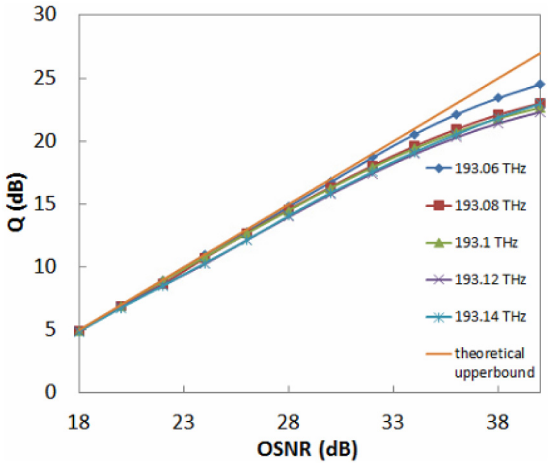

Fig. 11. Q vs. OSNR of 5-channel TDM of OFDM channels. The dispersion slopes of Fiber 3 and Fiber 5 are set to 0.092 ps/nm^2/km, and the dispersion slope of DF-HNLF A and DF-HNLF B are set to 0.006 ps/nm^2/km

As described in [15], third-order dispersion in the FWM chirp operation will lead to both temporal and spectral distortion because of imperfect mixing in the HNLFs. These distortions manifest as an asymmetric output idler spectrum, a timing shift and center frequency shift. In the dispersive fiber, third-order dispersion only affects the signal in the temporal domain.

#248812 Received 28 Aug 2015; revised 21 Oct 2015; accepted 28 Oct 2015; published 5 Nov 2015

Third-order dispersion results in temporal pulse asymmetry and blurred tail on one side of each pulse. This asymmetry in the time domain can be transferred to the spectral domain if the signal is to be subsequently processed in a time-lens; however, this seems to have only a minor effect on our system, compared with the distortions caused by TOD in DF-HNLFs A and B.

Figure 12 shows the spectra of the signal (Idler 2) at the output of a time-lens pair when DF-HNLF A has dispersion slope of 0.006 ps/nm^2/km and the dispersion slope of DF-HNLF B is zero (left), and conversely, where DF-HNLF B has dispersion slope of 0.006 ps/nm^2/km and DF-HNLF A has zero slope (right). A more severe asymmetry effect can be observed in Fig. 12(b), because the bandwidth of Pump 2 is five times broader than Pump 1, and so will be more heavily affected by third-order dispersion. From Fig. 12, we can infer that the frequency shift caused by third order dispersion is dominated by the first time-lens, and the asymmetry effect from TOD is dominated by the second time-lens.

The timing shift due to TOD in the time-lens pair results in an output frequency shift. The temporal shift generated in the first time-lens is converted to frequency shift in the second time-lens through time-to-frequency conversion, and it is multiplied by the conversion factor (i.e. the chirp rate of the second time-lens). For example, with a chirp rate of the second time-lens 4.6 × 10^{22} Hz/s, a dispersion slope in DF-HNLF A of 0.01 ps/nm^2/km results in a center frequency shift of 10 GHz. Delaying Pump 2 in order to temporally align the Idler 1 symbols and Pump 2 pulses can solve this issue. As such, the timing shift effect at the output of time-lens pair has a negligible impact compared with spectral shift and asymmetry.

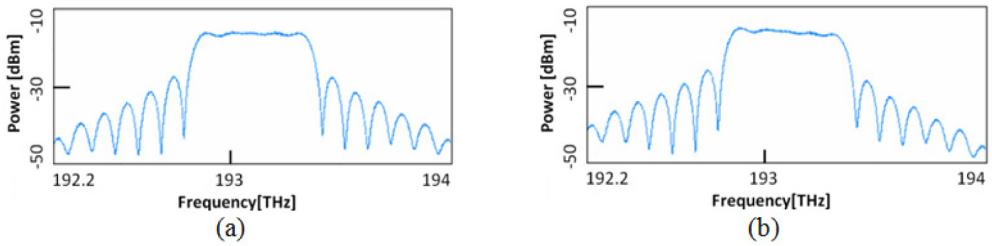

Fig. 12. Spectra of time-lens pair output in case of (a) dispersion slope of DF-HNLF A is 0.006 ps/(nm^2.km), other dispersion slopes are set to zero. (b) dispersion slope of DF-HNLF B is 0.006 ps/(nm^2.km), other dispersion slopes are set to zero.

6. Conclusion

In this paper, we investigated the impact of third-order-dispersion and nonlinear distortion on the performance of time-lens based communication systems for the first time, using metrics known to communications engineers. The penalties shown in this system stress the need for careful engineering of generic time-lens systems for optical signal processing. Penalties in time-lens systems are often notable, generally resulting in error floors [7, 22, 24].

To avoid error floors due to third-order dispersion in the highly nonlinear fiber, slope vales of <0.006 ps/(nm^{2}km) are required for pump bandwidths approaching or in excess of 1.3-THz. These bandwidths are required when the product of processing signal input bandwidths and spectral magnification factor is greater than 2.6 THz. If significantly lower pump bandwidths are allowed, more conventional HNLFs may be used.

To avoid error floors from nonlinear distortion, signal powers 20-dB lower than pump average powers are required to the signal causing nonlinear mixing. Note that this is well below the pump saturation level of the parametric mixer.

We have also highlighted some design considerations through our investigation, which may lead to improved performance in demonstrated time-lens systems. For example, if linearly chirped pump pulses with more-rectangular temporal profiles can be generated, a smaller temporal guard band is needed to accommodate effects from pump edges. The

#248812 Received 28 Aug 2015; revised 21 Oct 2015; accepted 28 Oct 2015; published 5 Nov 2015

nonlinear mixing stages should be engineered to ensure that TOD is low, and it may be desirable to utilize fiber Bragg gratings or spectral phase filters (such as LCOS based devices) to impart focal group delay dispersion without third-order aberrations. If the input signal is not broadband, reducing pump bandwidth may help to improve overall performance. Overall, we identified the dominant and minor degradation sources of time-lens based communication system, and our findings are applicable to a variety of all-optical signal processing functions.

We have shown through simulation the compression of 5 × 200 Gb/s, QPSK modulated OFDM channels into a single 1 Tb/s OTDM OFDM signal. Even in this highly demanding system, close to ideal operation can be achieved using parameters from off-the-shelf components, showing that this sub-system may be feasibly implemented. In summary, our work can give designers an indication of which equipment to select and the optimum pump and signal powers. This insight will speed experimental investigations for future time-lens research.

Acknowledgments

We thank VPIphotonics (www.vpiphotonics.com) for the use of their simulator, VPItransmissionMaker WDM V9.1. This work is supported under the Australian Research Council's Centre of Excellence CUDOS – Centre for Ultrahigh-bandwidth Devices for Optical Systems (CE110001018) and an ARC Laureate Fellowship (FL130100041).

#248812 Received 28 Aug 2015; revised 21 Oct 2015; accepted 28 Oct 2015; published 5 Nov 2015